Precipitation of Arsenic in Doped GaAs

C.L. CHANG, K. MAHALINGAM, and N. OTSUKA

School of Materials Engineering, Purdue University, W. Lafayette, IN 47907

M.R. MELLOCH

School of Electrical Engineering, Purdue University, W. Lafayette, IN 47907

J.M. WOODALL

IBM T.J. Watson Research Center, P.O. Box 218, Yorktown Heights, NY 10598

Precipitation processes in the p-type, n-type, and intrinsic GaAs layers grown by molecular beam epitaxy at a low temperature were studied by transmission electron microscopy. The average spacing, average diameter, and volume fraction of precipitates were measured as a function of the annealing time for the annealing temperature of 700°C. Volume fractions of precipitates are nearly constant in each layer over the period of annealing, implying that the precipitation process has reached the coarsening stage in the annealing times used in the study. The volume fraction of precipitates in the n-type layer is about a half of those in the p-type and intrinsic layers, suggesting that the incorporation rate of excess As into the n-type layer during the growth is lower than those into the p-type and intrinsic layers. Despite a large difference of amounts of excess As in as-grown n-type, p-type, and intrinsic layers, the average spacings and, hence, number densities of precipitates in three layers are nearly identical for each of the annealing conditions.

Key words: Arsenic, LT-GaAs, precipitation

GaAs epilayers grown by molecular beam epitaxy (MBE) at low substrate temperatures (200–250°C) were found to contain 1–2% excess arsenic.[1] Upon annealing at high temperatures, excess arsenic atoms form precipitates of the elemental arsenic phase.[2] The formation of arsenic precipitates during the annealing results in changes in material properties from those due to point defects (As interstitials and As antisites) to those due to the internal Schottky barriers associated with the arsenic precipitates.[3,4] A number of new electronic properties[5-7] as well as novel precipitation phenomena[8,9] have been observed from these GaAs layers containing As precipitates. As such observations, earlier studies found strong effects of impurity doping on precipitation processes of As in

GaAs.[10-13] In the p-n junction with Be and Si as dopants, excess As atoms migrate toward the n-type region, forming higher density precipitates in the n-type region than in the p-type region.[11] A particularly interesting observation made in that study is a direct correlation of the precipitate distribution with the electron states, i.e., Fermi level positions, which suggests that the precipitation process in doped GaAs may have fundamental differences from the conventional ones observed in metal systems. In this paper, we present a quantitative study of the precipitation processes in doped and intrinsic GaAs layers grown by MBE at a low temperature. In order to investigate the precipitation process in each layer without effects of migrations of excess As atoms from neighboring layers, thick n-type, p-type, and intrinsic layers were grown with a thin AlGaAs layer at each boundary.
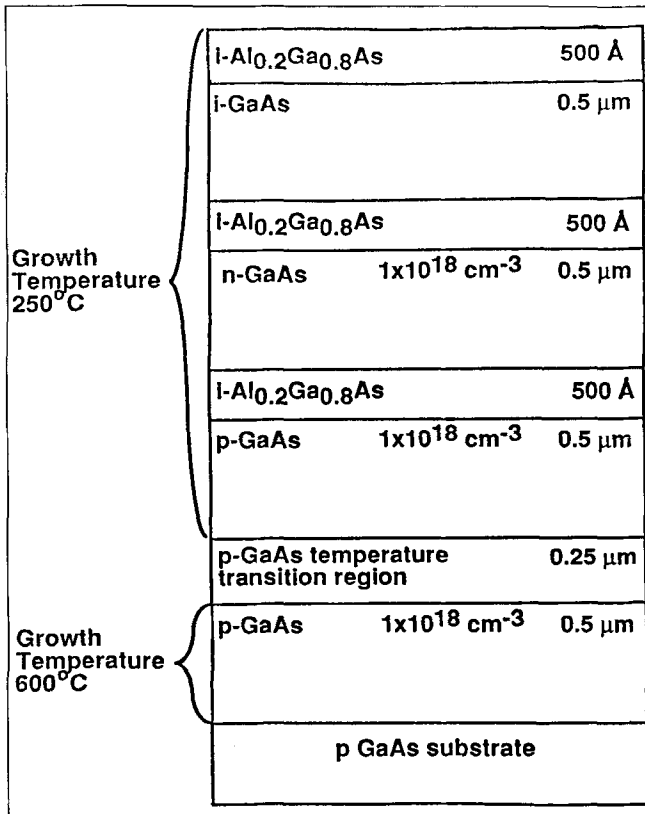
Fig. 1. Configuration of the p-n-i layer structure.

Fig. 3. (111) dark field image of the p-n-i layer structure annealed at 700°C for 10 h.
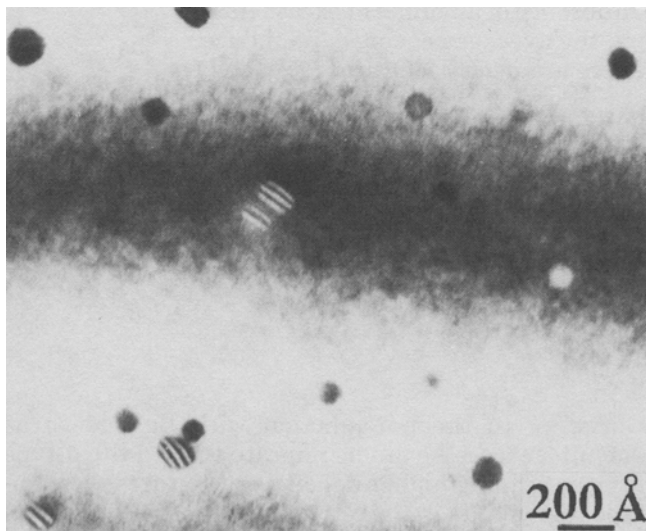
Fig. 2. (111) dark field image of the p-type region in the sample annealed at 700°C for 3 h.

The p-n-i layer structure used in this study was grown in a Varian GEN II MBE system. The configuration of the structure is shown in Fig. 1. The arsenic flux used was the dimer As_2, and Si and Be were used for the n-type and p-type dopants. All layers were grown at 250°C with a rate of 1 μm/h with a group V to group III beam-equivalent-pressure ratio of 20. The p-n-i layer structure was cut into a number of pieces and annealed at 700°C in an Ar gas flow for four different times, 5 min, 30 min, 3 h, and 10 h.
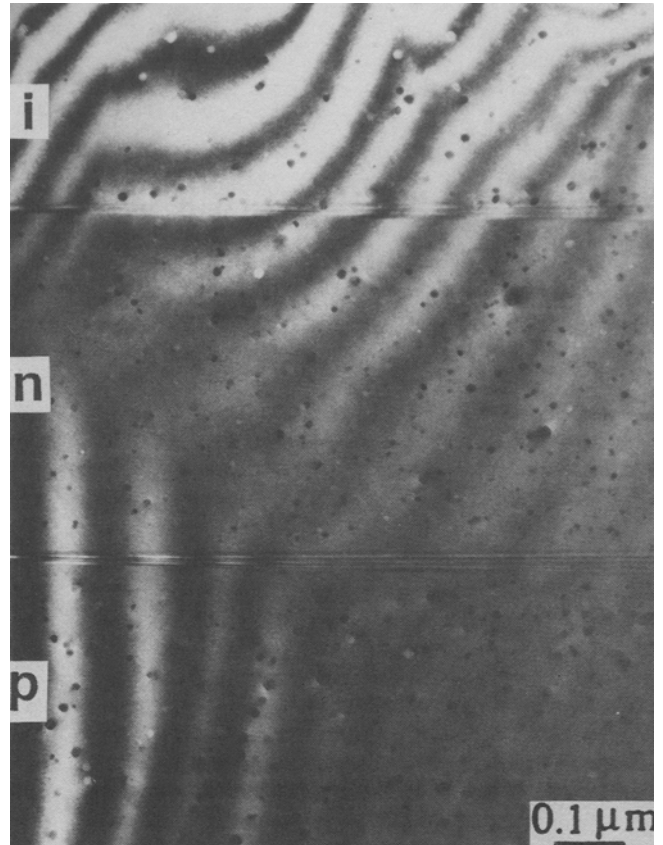
Transmission electron microscope (TEM) images of precipitates in annealed samples were obtained by observing cross-sectional specimens with a JEM 2000EX electron microscope. For the quantitative analysis of precipitate distributions, 111 and 220 dark field images were taken under the two-beam condition from each annealed sample.

The average diameter of precipitates was estimated by measuring sizes of nearly 200 precipitates in each region by using an Eyecon image analyzer. For this measurement, dark field images were taken at a magnification of 100, 000, and a diameter of each precipitate was determined by measuring two orthogonal directions and obtaining their average value. At this magnification, the majority of precipitates exhibit clear boundaries with the matrix in negatives of images. Figure 2 is an example of the image used for the measurement of precipitate diameters. The frequency distribution of precipitate diameters in each sample forms a single peak with the peak value being close to the average value. The standard deviations of measured diameters with respect to the average values, which correspond to broadening of peaks of frequency distributions, range from 11 to 23Å among samples. The average spacings of precipitates were determined by counting a number of precipitates in an area along an equal thickness contour of a dark field image. The volume of the area was estimated by using the extinction distance of the reflection used.

For each region, the average spacings of ten different areas were measured. The standard deviation of the average spacings obtained from ten areas ranges from 13 to 32Å. The number of precipitates in one measured area and the volume of the area are typically 15 and 2×10^9 Å^3, respectively. Volume fractions of precipitates were calculated by using the average diameters and the average spacings. Measured volume fractions may be significantly smaller than absolute values of volume fractions because of invisibility of a certain portion of precipitates in dark field images. In order to examine such a possibility, we have taken several dark field images using different reflections from the same area. By comparing those images, we found that almost all precipitates are visible in these dark field images although their contrasts vary from one image to another. Only a small portion of precipitates (a few percent) were found to be invisible when they were located at the centers of a dark thickness contours. The measured volume fractions of precipitates, therefore, are very close to the absolute values. We also would like to note that the imaging condition was kept identical in observations of all samples. The aforementioned problem, therefore, is not expected to affect the main findings of the present study.

Figure 3 is a 111 dark field image taken from the sample annealed at 700°C for 10 h. The image shows that sizes of precipitates in the n-type region are smaller than those in the p-type and intrinsic regions. Table I lists the average diameters of precipitates in three regions for four annealing times. It is seen from the table that the average diameter increases with increasing the annealing time in each region. For each annealing time, the average diameters of the p-type and intrinsic regions are close to each other, while that of the n-type region is significantly smaller than the others. Table II lists the average spacings of precipitates in three regions for four annealing times. In all regions, the average spacings increase with increasing the annealing time. The important point shown by this table is the nearly identical average spacings in three regions for each annealing time. The differences among the three regions are smaller than the standard deviations of measured values.

Table III lists volume fractions of precipitates. For each region, the volume fraction remains almost constant among different annealing times except for those of the p-type and intrinsic regions annealed at 5 min. The large deviation of these two values, 0.36 and 0.37%, from others is believed to be due to the difficulty in measuring precipitate diameters in the annealed samples where precipitates are still very small. The nearly constant volume fractions among four annealing times indicate that the precipitation process has already reached the coarsening stage in the 5 min annealing at this annealing temperature. This also implies that volume fractions of precipitates correspond to amounts of excess As in the as-grown layers because the nonstoichiometry of the matrix at the coarsening stage is considered to be close to the

nonstoichiometry of the crystal under the equilibrium condition. Volume fractions listed in Table III, hence, suggest that the amount of excess As in the n-type region is about a half of those in the p-type and intrinsic regions. There may be the possibility that all three regions originally have nearly identical amounts of excess arsenic but a smaller portion of excess arsenic has changed into precipitates in the n-type region than in the other two regions, leaving a significant amount of excess arsenic in the matrix of the n-type region. This possibility, however, is very unlikely because it implies that the Si-doped GaAs can have a significant degree of nonstoichiometry toward the As-rich side under the equilibrium condition. The smaller incorporation of excess As into the n-type layer may be explained by considering that excess As atoms become deep donors in GaAs.[11] The incorporation of a deep donor into the n-type region requires a greater energy than into the p-type and intrinsic regions. Smaller sizes of precipitates in the n-type regions than those in the p-type and intrinsic regions may be attributed to the difference in the amount of excess As and, hence, the difference of degrees of supersaturations in as-grown layers.

There are two important findings in the present study which require further examinations. The first one is nearly identical average spacings or nearly identical number densities of precipitates in three

Table I. Average Diameters of Precipitates in Three Regions for Four Annealing Times

Anlg. Time	Region		
	N-Type GaAs	P-Type GaAs	Intrinsic GaAs
5 min	52Å	68Å	70Å
30 min	64Å	79Å	79Å
3 h	73Å	90Å	88Å
10 h	82Å	102Å	103Å

Table II. Average Spacings of Precipitates in Three Regions for Four Annealing Times

Anlg. Time	Region		
	N-Type GaAs	P-Type GaAs	Intrinsic GaAs
5 min	357Å	356Å	364Å
30 min	447Å	439Å	442Å
3 h	491Å	504Å	490Å
10 h	557Å	560Å	568Å

Table III. Volume Fractions of Precipitates in Three Regions for Four Annealing Times

Anlg. Time	Region		
	N-Type GaAs	P-Type GaAs	Intrinsic GaAs
5 min	0.16%	0.36%	0.37%
30 min	0.15%	0.31%	0.30%
3 h	0.17%	0.30%	0.31%
10 h	0.16%	0.32%	0.31%

regions at each stage of the annealing. The close matching of average spacings at all four annealing times suggests that the matching is not merely accidental but results from a novel mechanism underlying the precipitation process in doped GaAs. The other finding is the rate constants of coarsening which correspond to a slope of the linear relation of the cube of average radius with the annealing time.[14] The rate constant of the n-type region is smaller than those in the p-type and intrinsic regions. This result forms a distinct contrast to the case of As precipitation in thin p-n junctions.[11] In thin p-n junctions, precipitates grow more rapidly in the n-type region at the expense of precipitates in the p-type region through migration of excess As atoms across the junction. The analysis of these two results will be reported in a separate paper.

ACKNOWLEDGMENT

REFERENCES

1. M. Kaminska, Z. Liliental-Weber, E.R. Weber, T. George, J.B. Kortright, F.W. Smith, B.Y. Tsaur and A.R. Calawa, *Appl. Phys. Lett.* 54, 1881 (1989).
2. M.R. Melloch, N. Otsuka, J.M. Woodall, A.C. Warren and J.L. Freeouf, *Appl. Phys. Lett.* 57,1531 (1990).
3. A.C. Warren, J.M. Woodall, J.L. Freeouf, D. Grischkowsky, D.T. McInturff, M.R. Melloch and N. Otsuka, *Appl. Phys. Lett.* 57, 1331 (1990).
4. A.C. Warren, J.M. Woodall, P.D. Kirchner, X. Yin, F. Pollack, M.R. Melloch, N. Otsuka and K. Mahalingam, *Phys. Rev. B* 46, 4617 (1992).
5. F.W. Smith, A.R. Calawa, C. Lee, M.J. Manfra and L.J. Mahoney, *IEEE Electron. Device Lett.* EDL-9, 77 (1988).
6. A.C. Warren, N. Katzenellenbogen, D. Grischkowsky, J.M. Woodall, M.R. Melloch and N. Otsuka, *Appl. Phys. Lett.* 58, 1512 (1991).
7. M.R. Melloch, D.D. Nolte, N. Otsuka, C.L. Chang and J.M. Woodall, to be published in *J. Vac. Sci. Technol.*
8. K. Mahalingam, N. Otsuka, M.R. Melloch, J.M. Woodall and A.C. Warren, *J. Vac. Sci. Technol.* B9, 2328 (1991).
9. K. Mahalingam, N. Otsuka, M.R. Melloch and J.M. Woodall, *Appl. Phys. Lett.* 60, 3253 (1992).
10. M.R. Melloch, N. Otsuka, K. Mahalingam, C.L. Chang, P.D. Kirchner, J.M. Woodall and A.C. Warren, *Appl. Phys. Lett.* 61, 13 (1992).
11. M.R. Melloch, N. Otsuka, K. Mahalingam, C.L. Chang, P.D. Kirchner, J.M. Woodall, D. Pettit, F. Cardone, A.C. Warren and D.D. Nolte, *J. Appl. Phys.* 72, 3509 (1992).
12. K.L. Kavanagh, J.C.P. Chang, P.D. Kirchner, A.C. Warren and J.M. Woodall, *Appl. Phys. Lett.* 62, 286 (1993).
13. J.P. Ibbetson, J.S. Speck, A.C. Gossard and U.K. Mishra, *Appl. Phys. Lett.* 62, 169 (1993).
14. I.M. Lifshitz and V.V. Slyozov, *J. Phys. Chem. Solids* 9, 35 (1961).